



# Certain analytical solutions of the concatenation model with a multiplicative white noise in optical fibers

Mehmet Ekici · Cansu Ali Sarmaşık

Received: 12 January 2024 / Accepted: 5 March 2024  
© The Author(s) 2024

**Abstract** In the presence of spatio-temporal dispersion, perturbation terms of the Hamiltonian type as well as multiplicative white noise, analytical investigation of the concatenation model having the Kerr law of nonlinearity is carried out in this work. The Cole–Hopf transformation and direct assumptions with arbitrary functions are utilized to determine several analytic solutions to the governing equation, including multi-wave, two solitary wave, breather, periodic cross kink, Peregrine-like rational, and three-wave solutions. The parameter constraints that serve as the requisite condition for the existence of these wave solutions are also identified. In order to explore and illustrate the propagation and dynamical behaviors of some solutions reported in this research, 3D graphics and their corresponding contour plots are included. Results of this paper may be useful for the experimental realization of certain nonlinear waves in optical fibers and further understanding of their propagation dynamics.

**Keywords** Breather · Multi-wave · Kink · Three-wave · Interaction · Peregrine · Concatenation · White noise

---

M. Ekici (✉)  
Department of Mathematics, Faculty of Science and Arts, Yozgat Bozok University, 66100 Yozgat, Turkey  
e-mail: ekici-m@hotmail.com

C. A. Sarmaşık  
Department of Mathematics, School of Graduate Studies, Yozgat Bozok University, 66100 Yozgat, Turkey  
e-mail: tedali0101@gmail.com

## 1 Introduction

Since the explanation of the nonlinear evolution equations (NLEEs) for certain nonlinear phenomena appearing in fluid dynamics, plasma astrophysics, optics, and various other fields, analytic solutions of the NLEEs have been the subjects of extensive investigations, recently yielding many significant and compelling results in the literature [1–23]. In this context, various nonlinear models, such as the extended Kadomtsev–Petviashvili (KP) equations in different dimensions [1, 2], the extended (3+1)-dimensional Ito equations [3, 4], the KdV–Calogero–Bogoyavlenskii–Schiff (KdV–CBS) and negative-order KdV–CBS models developed within the framework of (3+1)-dimensional equations [5], as well as a fifth-order nonlinear integrable equation [6], the time-dependent two members of the KP hierarchy [7], and various Boussinesq equations [8], were investigated to explore their integrability characteristics and to recover multiple-soliton solutions and other solutions. Using Hirota’s bilinear form, an examination and exploration were conducted to investigate lump solutions and collisions between lump and soliton solutions within the framework of the (3+1)-dimensional extended KP equation [9]. The Hirota–Satsuma–Ito equation underwent scrutiny employing the Hirota direct method, resulting in the discovery of multi-wave, breather wave, and interaction solutions for the model [10]. Localized solutions for the (2+1)-dimensional BKP equation were obtained [11]. The study of the (2+1)-dimensional

complex mKdV equation revealed the emergence of rogue waves, along with a discussion on modulation instability [12]. The examination of interaction solutions for the extended Jimbo–Miwa equation in (3+1) dimensions was conducted [13]. Lump solutions for a (3+1)-dimensional Boussinesq-type equation were revealed through the utilization of the long-wave limit approach, and simultaneously, interaction solutions were systematically formulated [14]. Hirota’s bilinear method was applied to investigate the generalized water wave equation, leading to the construction of lump and lump-type solutions for the examined model [15]. The investigation of a generalized Whitham–Broer–Kaup–Boussinesq–Kupershmidt system revealed that the system passed the Painlevé test, and both bilinear forms and  $N$ -soliton solutions of the system were obtained [16]. Two families of hetero-Bäcklund transformations, along with a family of similarity reductions, were developed for an extended coupled (2+1)-dimensional Burgers system [17]. The auto-Bäcklund transformations of an enlarged three-coupled KdV system were sought and yielded some solitons to the governing system [18]. By constructing a set of the similarity reductions, a (3+1)-dimensional generalized Yu–Toda–Sasa–Fukuyama system for certain interfacial waves in a two-layer liquid or elastic waves in a lattice was researched [19]. An investigation was carried out on a generalized Darboux transformation and solitons of the Ablowitz–Ladik equation [20]. The  $N$ -fold Darboux transformation (DT),  $N$ -fold generalized DT, and multi-pole soliton solutions of the system were reported as a result of the study conducted on a system for ultra-short pulses in an inhomogeneous multi-component nonlinear optical medium [21]. The exploration of auto-Bäcklund transformations was conducted for a (3+1)-dimensional Korteweg–de Vries–Calogero–Bogoyavlenskii–Schif equation in a fluid, uncovering soliton solutions to the model as well [22]. A (2+1)-dimensional generalized variable-coefficient Boiti–Leon–Pempinelli system was discussed, presenting two branches of the similarity reductions [23].

Solitons have been essentially described as the exceptional solutions of a particular class of the NLEEs, which may have variable or constant coefficients [24–51]. Several well-known NLEEs, such as nonlinear Schrödinger’s equation (NLSE), complex Ginzburg–Landau equation (CGLE), Sasa–Satsuma equation (SSE), Radhakrishnan–Kundu–Lakshmanan (RKL) equation, Lakshmanan–Porsezian–Daniel (LPD) model,

and others, describe the propagation of solitons through intercontinental optical fibers. The concatenation model, which combines the well-known NLSE with the LPD model and SSE, is a recent and interesting equation that was proposed in 2014 [24, 25]. The model underwent extensive research following its introduction and then for the model, optical solitons [26–28, 30, 32–34], Painlevé analysis [26], conservation laws [28], bifurcation analysis [29, 32], as well as chaotic behavior [29], quiescent optical solitons [31], implicit quiescent optical solitons [35], and dark solitary pulses and moving fronts [36] have been reported. Afterwards, the model was examined in birefringent fibers, and optical solitons [37–39], complexitons [39], and quiescent optical solitons [40] have also been discovered in that case. The presentation of the concatenation model having multiplicative white noise and the reporting of its soliton solutions have occurred very recently [41]. The aim of this research is to examine how multiplicative white noise affects the concatenation model. Several analytic solutions for the governing concatenation model are derived with the assistance of direct test functions and the Cole–Hopf transformation, and the associated constraint conditions for their existence are also provided. In particular, the results presented below demonstrate the richness of an optical fiber medium described by concatenation model, which is measured by the diversity of structures that it can support. This may have potential application for the further experiments and research in nonlinear optics. Following a brief presentation of the model, the details are enlisted in the subsequent sections of the paper.

## 1.1 Governing model

The stochastic concatenation model with the inclusion of perturbation terms is formulated as follows [41]:

$$\begin{aligned}
 & i q_t + a q_{xx} + b q_{xt} + c |q|^2 q \\
 & + d_1 \left[ \rho_1 q_{xxx} + \rho_2 (q_x)^2 q^* + \rho_3 |q_x|^2 q \right. \\
 & \left. + \rho_4 |q|^2 q_{xx} + \rho_5 q^2 q_{xx}^* + \rho_6 |q|^4 q \right] \\
 & + i d_2 \left[ \rho_7 q_{xxx} + \rho_8 |q|^2 q_x + \rho_9 q^2 q_x^* \right] \\
 & + \sigma (q - i b q_x) \frac{dW(t)}{dt}
 \end{aligned}$$

$$= i \left[ \alpha q_x + \lambda \left( |q|^2 q \right)_x + \mu \left( |q|^2 \right)_x q \right]. \tag{1}$$

Here the dependent variable  $q(x, t)$ , which characterizes the wave profile, is a complex-valued function, where  $x$  and  $t$  respectively stand for the spatial and temporal coordinates as two independent variables, while  $i = \sqrt{-1}$ . The linear temporal evolution is governed by the initial term, while the terms  $a, b$ , and  $c$  are the coefficients of chromatic dispersion (CD), spatio-temporal dispersion (STD), and the Kerr law of self-phase modulation (SPM), respectively. Next, the coefficient of  $d_1$  is associated with the LPD model, and the coefficient of  $d_2$  is sourced from the SSE. The role of  $\sigma$  is to signify the coefficient of noise strength, while  $W(t)$  corresponds to the standard Wiener process, and  $dW(t)/dt$  expresses the white noise. The parameters  $\alpha, \lambda$ , and  $\mu$  play a significant role as the coefficients of inter-modal dispersion, self-steepening effect, and self-frequency shift, respectively. It should also be noted here that in the case of  $d_1 = d_2 = 0$ , the governing model simplifies to the perturbed stochastic NLSE; however, if either  $d_1 = 0$  or  $d_2 = 0$ , it corresponds to the perturbed stochastic SSE or the perturbed stochastic LPD model, respectively. Thus, Eq. (1), which combines the perturbed stochastic versions of the NLSE, LPD model, and SSE, is referred to as the concatenation model.

As to the novelty of this study, it is recognized that multi-wave, two solitary wave, breather, periodic cross kink, Peregrine-like rational, and three-wave solutions for the perturbed stochastic concatenation model given by Eq. (1) have not been reported. As a result and hereby, it will make sense for us to explore multi-wave, two solitary wave, breather, periodic cross kink, Peregrine-like rational, and three-wave solutions to the governing equation (1). Therefore, the findings presented in the study are novel and reported here for the first time.

The content of this paper is as follows: In Sect. 2, Eq. (1) will be transformed into the desired form with the help of an assumption based on amplitude-phase format. Next, the Cole–Hopf transformation and three-wave hypothesis will be utilized to obtain multi-wave solutions in Sect. 3. In Sect. 4, interactional solutions will be investigated under the influence of the double exponential function assumption. The homoclinic breather approach will be employed to investigate breather wave solutions in Sect. 5. From Sect. 6–8, periodic cross kink, Peregrine-like rational, and three-

wave solutions will be derived by the implementation of various direct test functions. Finally, in Sect. 9, the results of the research will be outlined.

## 2 Mathematical setup

To carry out the integration of the governing equation (1), the employed hypothesis is

$$q(x, t) = P(\xi)e^{i\phi(x,t)} \tag{2}$$

where the wave variable is given by

$$\xi = x - vt. \tag{3}$$

The amplitude part is represented by the function  $P(x, t)$  and the soliton velocity is symbolized as  $v$ , according to the aforementioned hypothesis. Next, the phase component is presented with the structure

$$\phi = -\kappa x + \omega t + \sigma W(t) - \sigma^2 t + \theta. \tag{4}$$

Here  $\kappa$  stands for the frequency and  $\omega$  signifies the wave number, while  $\sigma$  corresponds to the noise coefficient and  $\theta$  denotes the phase constant. Substituting (2) into (1), one obtains the real part

$$\begin{aligned} & - \left[ \alpha \kappa + a \kappa^2 + (b \kappa - 1) (\sigma^2 - \omega) \right. \\ & \quad \left. + \kappa^3 (d_2 \rho_7 - d_1 \kappa \rho_1) \right] P \\ & + \left[ c - \kappa \lambda - d_1 \kappa^2 (\rho_2 - \rho_3 + \rho_4 + \rho_5) \right. \\ & \quad \left. + d_2 \kappa (\rho_8 - \rho_9) \right] P^3 \\ & + d_1 \rho_6 P^5 + d_1 (\rho_2 + \rho_3) P (P')^2 \\ & + (a - b v - 6 d_1 \kappa^2 \rho_1 + 3 d_2 \kappa \rho_7) P'' \\ & + d_1 (\rho_4 + \rho_5) P^2 P'' + d_1 \rho_1 P^{(4)} = 0 \end{aligned} \tag{5}$$

and the imaginary portion

$$\begin{aligned} & \left( v + \alpha + 2 a \kappa - b v \kappa + b \sigma^2 - b \omega - 4 d_1 \kappa^3 \rho_1 \right. \\ & \quad \left. + 3 d_2 \kappa^2 \rho_7 \right) P' \end{aligned}$$

$$\begin{aligned}
& + \left[ 3\lambda + 2\mu + 2d_1\kappa (\rho_2 + \rho_4 - \rho_5) \right. \\
& \left. - d_2 (\rho_8 + \rho_9) \right] P^2 P' \\
& + (4d_1\kappa\rho_1 - d_2\rho_7) P^{(3)} = 0.
\end{aligned} \tag{6}$$

From the imaginary equation given by (6), the velocity can be computed as

$$v = \frac{\alpha + 2a\kappa + b\sigma^2 - b\omega - 4d_1\kappa^3\rho_1 + 3d_2\kappa^2\rho_7}{b\kappa - 1} \tag{7}$$

with constraints

$$3\lambda + 2\mu + 2d_1\kappa (\rho_2 + \rho_4 - \rho_5) - d_2 (\rho_8 + \rho_9) = 0 \tag{8}$$

and

$$4d_1\kappa\rho_1 - d_2\rho_7 = 0. \tag{9}$$

Utilizing some abbreviations, Eq. (5) can be reformulated as follows:

$$\begin{aligned}
& M_1 P + M_2 P^3 + M_3 P^5 + M_4 P (P')^2 \\
& + M_5 P'' + M_6 P^2 P'' + P^{(4)} = 0
\end{aligned} \tag{10}$$

where

$$\begin{aligned}
M_1 &= -\frac{\alpha\kappa + a\kappa^2 + (b\kappa - 1)(\sigma^2 - \omega) + \kappa^3(d_2\rho_7 - d_1\kappa\rho_1)}{d_1\rho_1}, \\
M_2 &= \frac{c - \kappa\lambda - d_1\kappa^2(\rho_2 - \rho_3 + \rho_4 + \rho_5) + d_2\kappa(\rho_8 - \rho_9)}{d_1\rho_1}, \\
M_3 &= \frac{\rho_6}{\rho_1}, \quad M_4 = \frac{\rho_2 + \rho_3}{\rho_1}, \\
M_5 &= \frac{a - b\nu - 6d_1\kappa^2\rho_1 + 3d_2\kappa\rho_7}{d_1\rho_1}, \quad M_6 = \frac{\rho_4 + \rho_5}{\rho_1}.
\end{aligned} \tag{11}$$

Eq. (10) will now be examined to derive a variety of analytical solutions to the governing model.

### 3 Multi-wave solutions

By means of the transformation

$$P = 2 (\ln \psi)_\xi \tag{12}$$

one converts Eq. (10) into

$$\begin{aligned}
& M_1 \psi^4 \psi' + 2(2M_2 + M_5) \psi^2 (\psi')^3 \\
& + 4(4M_3 + M_4 + 2M_6 + 6) (\psi')^5 - 3M_5 \psi^3 \psi' \psi'' \\
& - 4(2M_4 + 3(M_6 + 5)) \psi (\psi')^3 \psi'' \\
& + 2(2M_4 + 15) \psi^2 \psi' (\psi'')^2 + M_5 \psi^4 \psi^{(3)} \\
& + 4(M_6 + 5) \psi^2 (\psi')^2 \psi^{(3)} - 10\psi^3 \psi'' \psi^{(3)} \\
& - 5\psi^3 \psi' \psi^{(4)} + \psi^4 \psi^{(5)} = 0.
\end{aligned} \tag{13}$$

The chosen assumption for deriving multi-wave solutions to the model is [42–46]:

$$\begin{aligned}
\psi &= \varrho_1 \cosh(\chi_1 \xi + \chi_2) + \varrho_2 \cos(\chi_3 \xi + \chi_4) \\
&+ \varrho_3 \cosh(\chi_5 \xi + \chi_6)
\end{aligned} \tag{14}$$

where  $\chi_j$  for  $1 \leq j \leq 6$  are constants. Substituting (14) into (13), collecting the coefficients of  $\sinh(\chi_1 \xi + \chi_2)$ ,  $\cosh(\chi_1 \xi + \chi_2)$ ,  $\sin(\chi_3 \xi + \chi_4)$ ,  $\cos(\chi_3 \xi + \chi_4)$ ,  $\sinh(\chi_5 \xi + \chi_6)$ ,  $\cosh(\chi_5 \xi + \chi_6)$ , and then working with the resulting system, one can uncover various sets of solutions.

(i) The first solution set is

$$\begin{aligned}
M_3 &= -\frac{M_1 + 4M_2\chi_1^2}{16\chi_1^4}, \\
M_5 &= \frac{M_1 + 4(M_4 + 4)\chi_1^4}{2\chi_1^2}, \quad M_6 \\
&= \frac{1}{8} \left( \frac{M_1}{\chi_1^4} + \frac{4M_2}{\chi_1^2} - 4(M_4 + 6) \right), \\
\chi_3 &= i\epsilon\chi_1, \quad \varrho_3 = 0.
\end{aligned} \tag{15}$$

The obtained results are inserted into (14), and the hypothesis (2) along with the transformation (12) are taken into account. Then, this process leads to deriving the rational multi-wave solution to the model (1) as

$$\begin{aligned}
 q(x, t) &= \frac{2\chi_1 [\varrho_1 \sinh(\chi_1 \xi + \chi_2) + \epsilon \varrho_2 \sinh(\epsilon \chi_1 \xi - i \chi_4)]}{\varrho_1 \cosh(\chi_1 \xi + \chi_2) + \varrho_2 \cosh(\epsilon \chi_1 \xi - i \chi_4)} \\
 &\quad \exp \left[ i \left( -\kappa x + \omega t + \sigma W(t) - \sigma^2 t + \theta \right) \right].
 \end{aligned} \tag{16}$$

This solution exists for  $\chi_4 = i\beta_1, \beta_1 \in \mathbb{R}$ .

(ii) The second solution set is

$$\begin{aligned}
 M_3 &= -\frac{M_1 + 4M_2\chi_1^2}{16\chi_1^4}, \\
 M_5 &= \frac{M_1 + 4(M_4 + 4)\chi_1^4}{2\chi_1^2}, \\
 M_6 &= \frac{1}{8} \left( \frac{M_1}{\chi_1^4} + \frac{4M_2}{\chi_1^2} - 4(M_4 + 6) \right), \\
 \chi_5 &= \epsilon \chi_1, \quad \varrho_2 = 0.
 \end{aligned} \tag{17}$$

These outcomes lead to the recovery of

$$\begin{aligned}
 q(x, t) &= \frac{2\chi_1 [\varrho_1 \sinh(\chi_1 \xi + \chi_2) + \epsilon \varrho_3 \sinh(\epsilon \chi_1 \xi + \chi_6)]}{\varrho_1 \cosh(\chi_1 \xi + \chi_2) + \varrho_3 \cosh(\epsilon \chi_1 \xi + \chi_6)} \\
 &\quad \exp \left[ i \left( -\kappa x + \omega t + \sigma W(t) - \sigma^2 t + \theta \right) \right].
 \end{aligned} \tag{18}$$

---


$$\begin{aligned}
 q(x, t) &= \frac{2\chi_5 [\varrho_1 \sinh(\chi_5 \xi + \chi_2) + \epsilon \varrho_2 \sinh(\epsilon \chi_5 \xi - i \chi_4) + \varrho_3 \sinh(\chi_5 \xi + \chi_6)]}{\varrho_1 \cosh(\chi_5 \xi + \chi_2) + \varrho_2 \cosh(\epsilon \chi_5 \xi - i \chi_4) + \varrho_3 \cosh(\chi_5 \xi + \chi_6)} \\
 &\quad \exp \left[ i \left( -\kappa x + \omega t + \sigma W(t) - \sigma^2 t + \theta \right) \right]
 \end{aligned} \tag{22}$$

(iii) The third solution set is

$$\begin{aligned}
 M_3 &= -\frac{M_1 - 4M_2\chi_3^2}{16\chi_3^4}, \\
 M_5 &= -\frac{M_1 + 4(M_4 + 4)\chi_3^4}{2\chi_3^2}, \quad M_6 \\
 &= \frac{1}{8} \left( \frac{M_1}{\chi_3^4} - \frac{4M_2}{\chi_3^2} - 4(M_4 + 6) \right), \\
 \chi_5 &= i\epsilon \chi_3, \quad \varrho_1 = 0.
 \end{aligned} \tag{19}$$

Considering these results, the subsequent solution to the governing equation is formulated as

$$\begin{aligned}
 q(x, t) &= -\frac{2\chi_3 [\varrho_2 \sin(\chi_3 \xi + \chi_4) + \epsilon \varrho_3 \sin(\epsilon \chi_3 \xi - i \chi_6)]}{\varrho_2 \cos(\chi_3 \xi + \chi_4) + \varrho_3 \cos(\epsilon \chi_3 \xi - i \chi_6)} \\
 &\quad \exp \left[ i \left( -\kappa x + \omega t + \sigma W(t) - \sigma^2 t + \theta \right) \right].
 \end{aligned} \tag{20}$$

The existence condition for this solution is  $\chi_6 = i\beta_2, \beta_2 \in \mathbb{R}$ .

(iv) The fourth solution set is

$$\begin{aligned}
 M_3 &= -\frac{M_1 + 4M_2\chi_5^2}{16\chi_5^4}, \\
 M_5 &= \frac{M_1 + 4(M_4 + 4)\chi_5^4}{2\chi_5^2}, \\
 M_6 &= \frac{1}{8} \left( \frac{M_1}{\chi_5^4} + \frac{4M_2}{\chi_5^2} - 4(M_4 + 6) \right), \\
 \chi_1 &= \chi_5, \quad \chi_3 = i\epsilon \chi_5.
 \end{aligned} \tag{21}$$

Under this circumstance, the rational multi-wave solution takes form as

which introduces the constraint  $\chi_4 = i\beta_1, \beta_1 \in \mathbb{R}$ . Also, it should be pointed out that  $\epsilon$  equals  $\pm 1$  in all solution sets.

Figure 1 illustrates the dynamical properties of rational multi-waves solution (22). In the (x, t)-plane, Fig. 1a, b, and c depict the 3D graphs, while Fig. 1d, e, and f enumerate the corresponding contour diagrams of Fig. 1a, b, and c. The chosen parameter values are  $v = 3.4, \epsilon = -1, \theta = 5, \kappa = 1.5, \varrho_1 = 5, \varrho_2 = 2, \varrho_3 = 7, \chi_2 = 9, \chi_4 = 12i, \chi_6 = 3, W(t) = \frac{\sigma}{2}t$  when  $\sigma = 0, \chi_5 = 2.6, \omega = 0.5$  in (a) and (d),  $\sigma = 3, \chi_5 = 0.2, \omega = 2.5$  in (b) and (e),

$\sigma = 10$ ,  $\chi_5 = -0.1$ ,  $\omega = 5.8$  in (c) and (f). The graphical presentation of the multi-wave solution given by Eq. (22) is depicted in Fig. 1. The influence of the noise effect  $\sigma$  and the parameters  $\chi_5$  and  $\omega$  on the behavior of the solution is examined, as can be seen from the chosen parameter values. It should be noted that Fig. 1a and d are simulated in the case of ( $\sigma = 0$ ), while Fig. 1b, c, e, and f are depicted in the case of  $\sigma \neq 0$ . Also, the examination range for these graphics is set as  $-5 \leq x \leq 5$  and  $-5 \leq t \leq 5$ .

#### 4 Exponential form

When recovering interactional solutions, the double exponential function is picked as follows [44–46]:

$$\psi = \varrho_1 \exp(\chi_1 \xi + \chi_2) + \varrho_2 \exp(\chi_3 \xi + \chi_4) \quad (23)$$

where  $\chi_j$  with  $1 \leq j \leq 4$  are constants. Putting (23) into (13) and subsequently setting the coefficients

Set-2.

$$\begin{aligned} M_1 &= \frac{16}{9} M_3 \chi_1^4 \left[ 32 M_3 (4 M_3 - 3) + 9 \right. \\ &\quad \left. + 8 (3 - 8 M_3) \sqrt{M_3 (4 M_3 - 3)} \right], \\ M_2 &= -\frac{8}{9} M_3 (8 M_3 - 3) \chi_1^2 \\ &\quad \left[ 8 M_3 - 3 - 4 \sqrt{M_3 (4 M_3 - 3)} \right], \\ M_4 &= 12 (M_3 - 1), \quad M_5 = -\frac{4}{9} (4 M_3 - 9) \chi_1^2 \\ &\quad \left[ 8 M_3 - 3 - 4 \sqrt{M_3 (4 M_3 - 3)} \right], \\ M_6 &= 3 - 8 M_3, \quad \chi_3 = \frac{1}{3} \chi_1 \\ &\quad \left[ 3 - 8 M_3 + 4 \sqrt{M_3 (4 M_3 - 3)} \right]. \end{aligned} \quad (26)$$

The solution derived from the second set of parameters for the model in question is

$$\begin{aligned} q(x, t) &= \frac{2 \chi_1 \left[ 3 \varrho_1 \exp(\chi_1 \xi + \chi_2) + \varrho_2 (3 - 8 M_3 + 4 \sqrt{M_3 (4 M_3 - 3)}) \exp\left(\frac{1}{3} [3 - 8 M_3 + 4 \sqrt{M_3 (4 M_3 - 3)}] \chi_1 \xi + \chi_4\right) \right]}{3 \left[ \varrho_1 \exp(\chi_1 \xi + \chi_2) + \varrho_2 \exp\left(\frac{1}{3} [3 - 8 M_3 + 4 \sqrt{M_3 (4 M_3 - 3)}] \chi_1 \xi + \chi_4\right) \right]} \\ &\quad \times \exp \left[ i \left( -\kappa x + \omega t + \sigma W(t) - \sigma^2 t + \theta \right) \right]. \end{aligned} \quad (27)$$

of  $\exp(\chi_1 \xi + \chi_2)$ ,  $\exp(\chi_3 \xi + \chi_4)$ , and other terms to zero, the following sets of solutions are identified by overcoming the resulting system of equations:  
Set-1.

$$\begin{aligned} M_1 &= 2 \chi_1^2 \left[ M_5 + 4 (2 M_3 + M_6 + 1) \chi_1^2 \right], \\ M_2 &= -\frac{M_5}{2} - 2 (4 M_3 + M_6 + 1) \chi_1^2, \\ M_4 &= -2 (2 M_3 + M_6 + 3), \quad \chi_3 = -\chi_1. \end{aligned} \quad (24)$$

Utilizing these parameter values within (23), and considering (2) along with (12), the multi-wave interactional solution is revealed as follows:

$$\begin{aligned} q(x, t) &= \frac{2 \chi_1 \left[ \varrho_1 \exp(\chi_1 \xi + \chi_2) - \varrho_2 \exp(\chi_4 - \chi_1 \xi) \right]}{\varrho_1 \exp(\chi_1 \xi + \chi_2) + \varrho_2 \exp(\chi_4 - \chi_1 \xi)} \\ &\quad \exp \left[ i \left( -\kappa x + \omega t + \sigma W(t) - \sigma^2 t + \theta \right) \right]. \end{aligned} \quad (25)$$

This solitary wave solution will exist provided  $M_3 (4 M_3 - 3) > 0$  holds.

The dynamic behaviors of Solution (27) are displayed in Fig. 2. In the (x, t)-plane, Fig. 2a, b, and c demonstrate the 3D graphs, while Fig. 2d, e, and f are the corresponding contour diagrams of Fig. 2a, b, and c. The picked parameter values are  $v = 0.7$ ,  $\theta = 1$ ,  $\kappa = 1.5$ ,  $\varrho_1 = 2$ ,  $\varrho_2 = 5$ ,  $\chi_2 = 3$ ,  $\chi_4 = -4$ ,  $M_3 = 1.4$ ,  $W(t) = \frac{\sigma}{2} t$  when  $\sigma = 0$ ,  $\chi_1 = -1.5$ ,  $\omega = 9$  in (a) and (d),  $\sigma = 4$ ,  $\chi_1 = -0.9$ ,  $\omega = 6$  in (b) and (e),  $\sigma = 10$ ,  $\chi_1 = -3.5$ ,  $\omega = 25$  in (c) and (f). The interaction phenomenon of two solitary waves, as depicted by Fig. 2, is discussed along with the influence of the noise effect  $\sigma$  and the parameters  $\chi_1$  and  $\omega$  on the behavior of the solution. Also, the examination range is set as  $-5 \leq x \leq 5$  and  $-5 \leq t \leq 5$ .

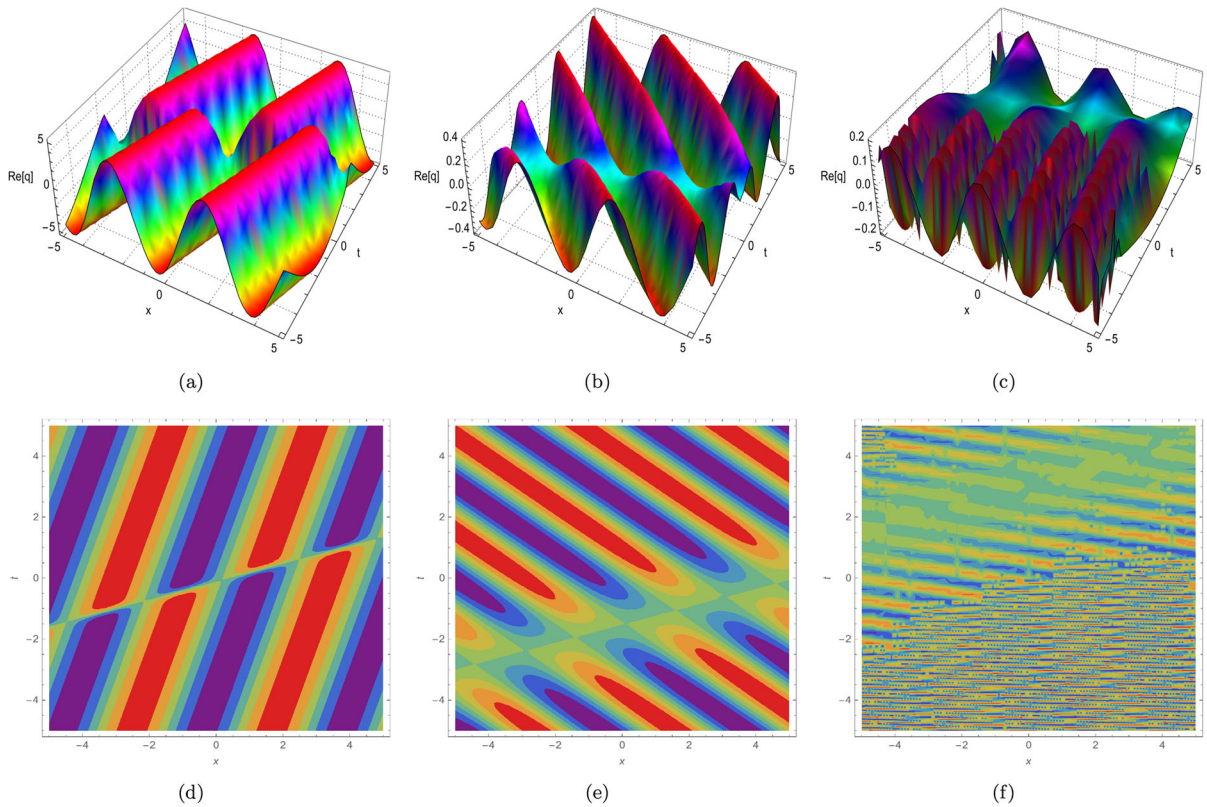


**Fig. 1** Dynamical behavior of solution (22)

**5 Homoclinic breather approach**

Breather wave hypothesis is represented by [42–44]

$$\psi = \exp[-\varpi (\chi_1\xi + \chi_2)] + \varrho_1 \exp[\varpi (\chi_3\xi + \chi_4)] + \varrho_2 \cos[\varpi_1 (\chi_5\xi + \chi_6)] \tag{28}$$

or equivalently

$$\psi = \sinh[-\varpi (\chi_1\xi + \chi_2)] + \cosh[-\varpi (\chi_1\xi + \chi_2)] + \varrho_1 \sinh[\varpi (\chi_3\xi + \chi_4)] + \varrho_1 \cosh[\varpi (\chi_3\xi + \chi_4)] + \varrho_2 \cos[\varpi_1 (\chi_5\xi + \chi_6)] \tag{29}$$

where  $\chi_j$  ( $1 \leq j \leq 6$ ) are constants. Inserting (29) into (13), collecting the coefficients of each

power of  $\sinh[\varpi (\chi_1\xi + \chi_2)]$ ,  $\cosh[\varpi (\chi_1\xi + \chi_2)]$ ,  $\sinh[\varpi (\chi_3\xi + \chi_4)]$ ,  $\cosh[\varpi (\chi_3\xi + \chi_4)]$ ,  $\sin[\varpi_1 (\chi_5\xi + \chi_6)]$ ,  $\cos[\varpi_1 (\chi_5\xi + \chi_6)]$ , as well as other terms, and solving the system of coefficients yields the following:

(i) The first set is

$$\begin{aligned} M_2 &= (M_4 + 2M_6 + 6) \chi_1^2 \varpi^2 - \frac{M_1}{4\chi_1^2 \varpi^2}, \\ M_3 &= -\frac{1}{4} [M_4 + 2(M_6 + 3)], \\ M_5 &= \frac{M_1 + 4(M_4 + 4) \chi_1^4 \varpi^4}{2\chi_1^2 \varpi^2}, \\ \varrho_1 &= 0, \quad \chi_5 = \frac{i\epsilon \chi_1 \varpi}{\varpi_1}. \end{aligned} \tag{30}$$

By substituting (30) into (29), and employing (2) along with (12), the breather solution emerges as

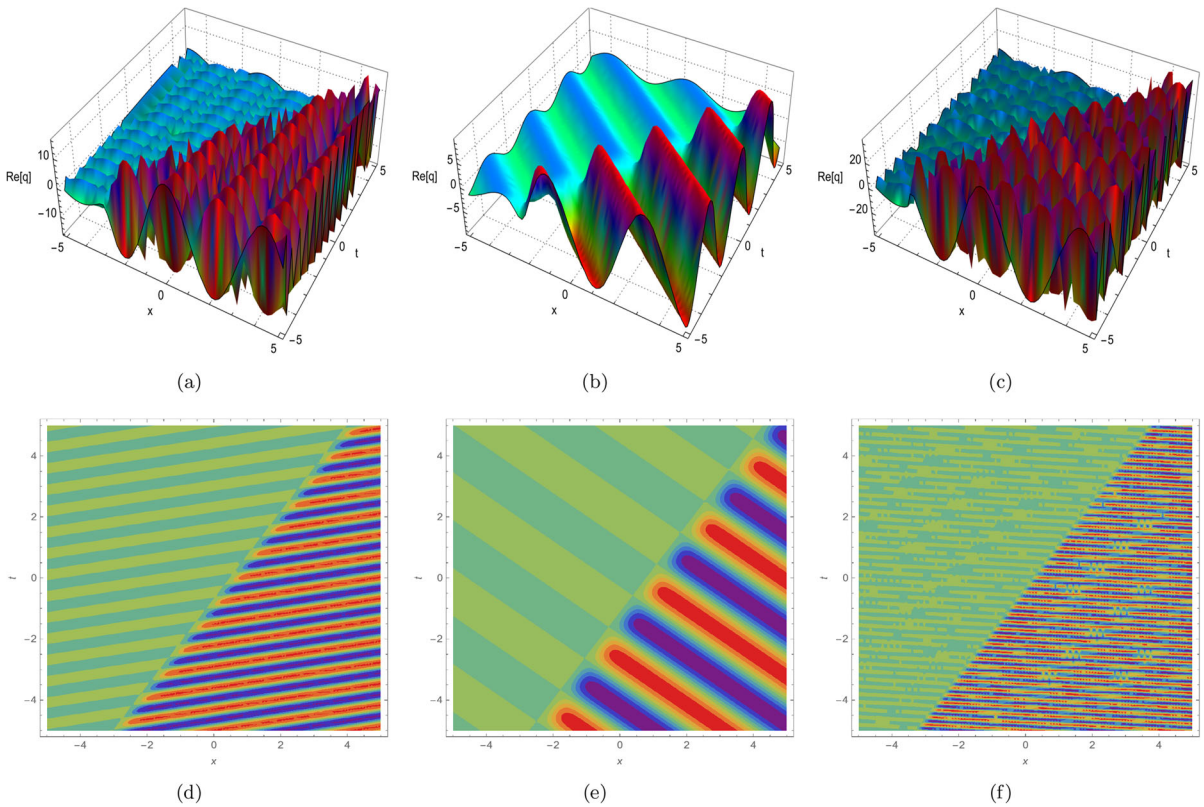


**Fig. 2** Dynamical behavior of solution (27)

$$q(x, t) = \frac{2\chi_1\varpi [\epsilon\varrho_2 \exp[\varpi (\chi_1\xi + \chi_2)] \sinh (\epsilon\chi_1\varpi\xi - i\chi_6\varpi_1) - 1]}{\varrho_2 \exp[\varpi (\chi_1\xi + \chi_2)] \cosh (\epsilon\chi_1\varpi\xi - i\chi_6\varpi_1) + 1} \exp \left[ i \left( -\kappa x + \omega t + \sigma W(t) - \sigma^2 t + \theta \right) \right]. \tag{31}$$

(ii) The second set is

$$M_2 = -\frac{13M_1 + 280\chi_1^4\varpi^4}{66\chi_1^2\varpi^2},$$

$$M_3 = \frac{7}{528} \left( 80 - \frac{M_1}{\chi_1^4\varpi^4} \right),$$

$$M_4 = \frac{8}{3} - \frac{7M_1}{12\chi_1^4\varpi^4},$$

$$M_5 = \frac{2(20\chi_1^4\varpi^4 - M_1)}{3\chi_1^2\varpi^2},$$

$$M_6 = \frac{7M_1}{22\chi_1^4\varpi^4} - \frac{71}{11},$$

$$\chi_3 = \chi_1, \quad \chi_5 = \frac{i\epsilon\chi_1\varpi}{\varpi_1}. \tag{32}$$

Continuing in the same manner, the following solution is established:



$$q(x, t) = \frac{2\chi_1\varpi [-\exp[-\varpi(\chi_1\xi + \chi_2)] + \varrho_1 \exp[\varpi(\chi_1\xi + \chi_4)] + \epsilon\varrho_2 \sinh(\epsilon\chi_1\varpi\xi - i\chi_6\varpi_1)]}{\exp[-\varpi(\chi_1\xi + \chi_2)] + \varrho_1 \exp[\varpi(\chi_1\xi + \chi_4)] + \varrho_2 \cosh(\epsilon\chi_1\varpi\xi - i\chi_6\varpi_1)} \times \exp\left[i\left(-\kappa x + \omega t + \sigma W(t) - \sigma^2 t + \theta\right)\right]. \tag{33}$$

Here, in all sets of solutions,  $\epsilon = \pm 1$ . It should also be emphasized that the solutions provided by Eqs. (31) and (33) are valid for  $\chi_6 = i\beta, \beta \in \mathbb{R}$ .

Figure 3 presents the physical structure of breather solution (33). In the  $(x, t)$ -plane, Fig. 3a, b, and c show the 3D graphs, while Fig. 3a, e, and f list the corresponding contour diagrams of Fig. 3a, b, and c. The chosen parameter values are  $v = 1.5, \epsilon = -1, \theta = 1, \kappa = 2, \varpi = 2.4, \varpi_1 = 3, \varrho_1 = 3, \varrho_2 = -7, \chi_2 = 9, \chi_4 = 2, \chi_6 = 5i, W(t) = \frac{\sigma}{2}t$  when  $\sigma = 0, \chi_1 = -0.7, \omega = 1.2$  in (a) and (d),  $\sigma = 5, \chi_1 = -0.9, \omega = 3.6$  in (b) and (e),  $\sigma = 10, \chi_1 = 1.7, \omega = 6.3$  in (c) and (f). The dynamical behavior of breather waves provided by Eq. (33) is displayed in Fig. 3. Considering the same examination range in Sects. 3 and 4, the graphical presentations for the case  $\sigma = 0$  are demonstrated in Fig. 3a and d, while Figs. 3b, c, e, and f stand for the case  $\sigma \neq 0$ . The influence of the parameters  $\chi_1$  and  $\omega$  on the behavior of the solution is also investigated.

### 6 Periodic cross kink solution

The derivation of a periodic cross kink solution to the concatenation model with multiplicative white noise is enabled by the following assumption [47,48]:

$$\psi = \exp(\chi_1\xi + \chi_2) + \varrho_1 \exp[-(\chi_1\xi + \chi_2)] + \varrho_2 \cos(\chi_3\xi + \chi_4) + \varrho_3 \cosh(\chi_5\xi + \chi_6) + \varrho_4 \tag{34}$$

where  $\chi_j$  for  $1 \leq j \leq 6$  are constants. Plugging (34) into (13), collecting the coefficients of

$\exp(\chi_1\xi + \chi_2), \exp[-(\chi_1\xi + \chi_2)], \cos(\chi_3\xi + \chi_4), \sin(\chi_3\xi + \chi_4), \cosh(\chi_5\xi + \chi_6), \sinh(\chi_5\xi + \chi_6)$ , and other terms, setting them equal to zero, and solving the resulting system leads to:

Case-1.

$$\begin{aligned} M_2 &= -\frac{M_1 + 16M_3\chi_1^4}{4\chi_1^2}, \\ M_5 &= \frac{M_1 + 4(M_4 + 4)\chi_1^4}{2\chi_1^2}, \\ M_6 &= -2M_3 - \frac{M_4}{2} - 3, \\ \varrho_1 = \varrho_2 = \varrho_4 &= 0, \quad \chi_5 = \epsilon\chi_1. \end{aligned} \tag{35}$$

Based on these outcomes, one secures the solution

$$q(x, t) = \frac{2\chi_1 [\exp(\chi_1\xi + \chi_2) + \epsilon\varrho_3 \sinh(\epsilon\chi_1\xi + \chi_6)]}{\exp(\chi_1\xi + \chi_2) + \varrho_3 \cosh(\epsilon\chi_1\xi + \chi_6)} \exp\left[i\left(-\kappa x + \omega t + \sigma W(t) - \sigma^2 t + \theta\right)\right]. \tag{36}$$

Case-2.

$$\begin{aligned} M_2 &= -\frac{M_1 + 16M_3\chi_1^4}{4\chi_1^2}, \\ M_5 &= \frac{M_1 + 4(M_4 + 4)\chi_1^4}{2\chi_1^2}, \\ M_6 &= -2M_3 - \frac{M_4}{2} - 3, \quad \varrho_2 = \varrho_4 = 0, \\ \chi_5 &= \epsilon\chi_1. \end{aligned} \tag{37}$$

In this case, the solution is expressed as

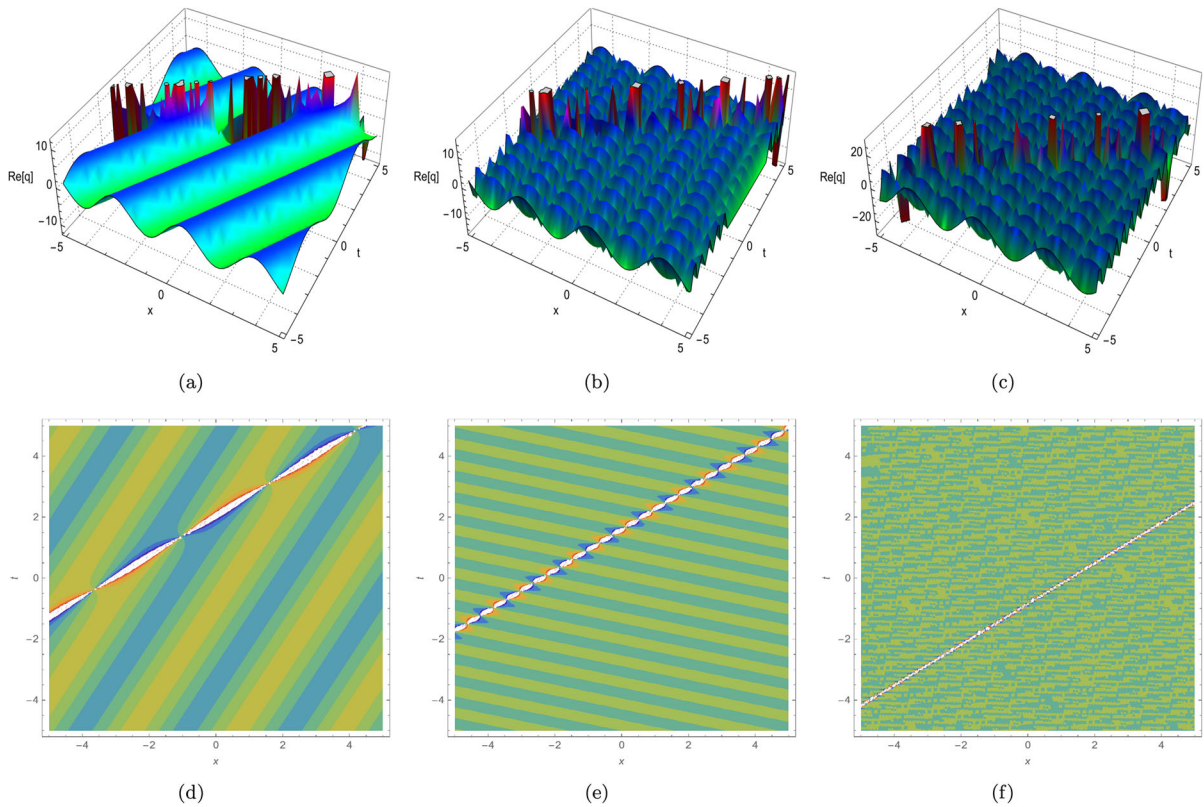


**Fig. 3** Dynamical behavior of solution (33)

$$q(x, t) = \frac{2\chi_1 [\exp(\chi_1\xi + \chi_2) [\exp(\chi_1\xi + \chi_2) + \epsilon\varrho_3 \sinh(\epsilon\chi_1\xi + \chi_6)] - \varrho_1]}{\exp(\chi_1\xi + \chi_2) [\exp(\chi_1\xi + \chi_2) + \varrho_3 \cosh(\epsilon\chi_1\xi + \chi_6)] + \varrho_1} \exp\left[i\left(-\kappa x + \omega t + \sigma W(t) - \sigma^2 t + \theta\right)\right]. \tag{38}$$

Case-3.

$$M_2 = -\frac{M_1 + 16M_3\chi_1^4}{4\chi_1^2},$$

$$M_5 = \frac{M_1 + 4(M_4 + 4)\chi_1^4}{2\chi_1^2},$$

$$M_6 = -2M_3 - \frac{M_4}{2} - 3,$$

$$\varrho_1 = \varrho_4 = 0, \quad \chi_3 = i\chi_1, \quad \chi_5 = \epsilon\chi_1. \tag{39}$$

This in turn gives rise to

$$q(x, t) = \frac{2\chi_1 [\exp(\chi_1\xi + \chi_2) + \varrho_2 \sinh(\chi_1\xi - i\chi_4) + \epsilon\varrho_3 \sinh(\epsilon\chi_1\xi + \chi_6)]}{\exp(\chi_1\xi + \chi_2) + \varrho_2 \cosh(\chi_1\xi - i\chi_4) + \varrho_3 \cosh(\epsilon\chi_1\xi + \chi_6)} \exp\left[i(-\kappa x + \omega t + \sigma W(t) - \sigma^2 t + \theta)\right]. \tag{40}$$

Case-4.

$$M_2 = -\frac{M_1 + 16M_3\chi_1^4}{4\chi_1^2}, \quad M_5 = \frac{M_1 + 4(M_4 + 4)\chi_1^4}{2\chi_1^2},$$

$$M_6 = -2M_3 - \frac{M_4}{2} - 3, \quad \varrho_4 = 0, \quad \chi_3 = i\chi_1,$$

$$\chi_5 = \epsilon\chi_1. \tag{41}$$

By the help of this set of parameters, it is discovered that

where  $\chi_j$  with  $1 \leq j \leq 5$  are constants. Inserting (43) into (13) yields the following results:

$$(i) \quad M_1 = 0, \quad M_3 = -\frac{1}{32}(2M_4 + 4M_6 + 3),$$

$$M_5 = -8M_2,$$

$$q(x, t) = \frac{2\chi_1 [\exp(\chi_1\xi + \chi_2) [\exp(\chi_1\xi + \chi_2) + \varrho_2 \sinh(\chi_1\xi - i\chi_4) + \epsilon\varrho_3 \sinh(\epsilon\chi_1\xi + \chi_6)] - \varrho_1]}{\exp(\chi_1\xi + \chi_2) [\exp(\chi_1\xi + \chi_2) + \varrho_2 \cosh(\chi_1\xi - i\chi_4) + \varrho_3 \cosh(\epsilon\chi_1\xi + \chi_6)] + \varrho_1} \times \exp\left[i(-\kappa x + \omega t + \sigma W(t) - \sigma^2 t + \theta)\right]. \tag{42}$$

In all solution sets presented here,  $\epsilon$  equals  $\pm 1$ . Also, it is important to highlight that the solutions (40) and (42) will exist as long as the considered equation satisfies the condition  $\chi_4 = i\beta$  ( $\beta \in \mathbb{R}$ ), which stands as the requisite condition for the existence of solutions. The propagation characteristics of Solution (42) are illustrated in Fig. 4. In the  $(x, t)$ -plane, Fig. 4a, b, and c demonstrate the 3D graphs, while Fig. 4d, e, and f are the corresponding contour diagrams of Fig. 4a, b, and c. The parameter values that are taken in this case are  $v = 0.8$ ,  $\epsilon = -1$ ,  $\theta = 1$ ,  $\kappa = 0.5$ ,  $\varrho_1 = -7.5$ ,  $\varrho_2 = 3.9$ ,  $\varrho_3 = -25.8$ ,  $\chi_2 = 6$ ,  $\chi_4 = 17i$ ,  $\chi_6 = 5$ ,  $W(t) = \frac{\sigma}{2}t$  when  $\sigma = 0$ ,  $\chi_1 = 2.6$ ,  $\omega = 3.7$  in (a) and (d),  $\sigma = 4$ ,  $\chi_1 = 5.2$ ,  $\omega = 43$  in (b) and (e),  $\sigma = 10$ ,  $\chi_1 = -1.9$ ,  $\omega = 41$  in (c) and (f). The dynamic behaviors of the periodic cross kink solution (42) are analyzed for various values of the parameters  $\sigma$ ,  $\chi_1$ , and  $\omega$ .

### 7 Peregrine-like rational solitons

The adopted assumption for this solution form is [45, 49]

$$\psi = (\chi_1\xi + \chi_2)^2 + (\chi_3\xi + \chi_4)^2 + \chi_5 \tag{43}$$

$$\chi_5 = -\frac{(\chi_2\chi_3 - \chi_1\chi_4)^2}{\chi_1^2 + \chi_3^2}. \tag{44}$$

Using these results in (43), and considering (2) along with (12) brings about the solution

$$q(x, t) = \frac{4(\chi_1^2 + \chi_3^2)}{\chi_1^2\xi + \chi_3(\chi_3\xi + \chi_4) + \chi_1\chi_2} \exp\left[i(-\kappa x + \omega t + \sigma W(t) - \sigma^2 t + \theta)\right]. \tag{45}$$

$$(ii) \quad M_1 = 0, \quad M_3 = -\frac{1}{32}(2M_4 + 4M_6 + 3), \quad M_5 = -8M_2, \quad \chi_2 = -\frac{\chi_3\chi_4}{\chi_1},$$

$$\chi_5 = -\frac{(\chi_1^2 + \chi_3^2)\chi_4^2}{\chi_1^2}. \tag{46}$$

From these results, one explores

$$q(x, t) = \frac{4}{\xi} \exp\left[i(-\kappa x + \omega t + \sigma W(t) - \sigma^2 t + \theta)\right]. \tag{47}$$

$$(iii) \quad M_1 = 0,$$

$$M_3 = \frac{1}{8} \left[ 3 - M_2 \left( \frac{2\chi_4^2}{\chi_1^2} + \frac{2\chi_5}{\chi_1^2 + \chi_3^2} \right) \right],$$

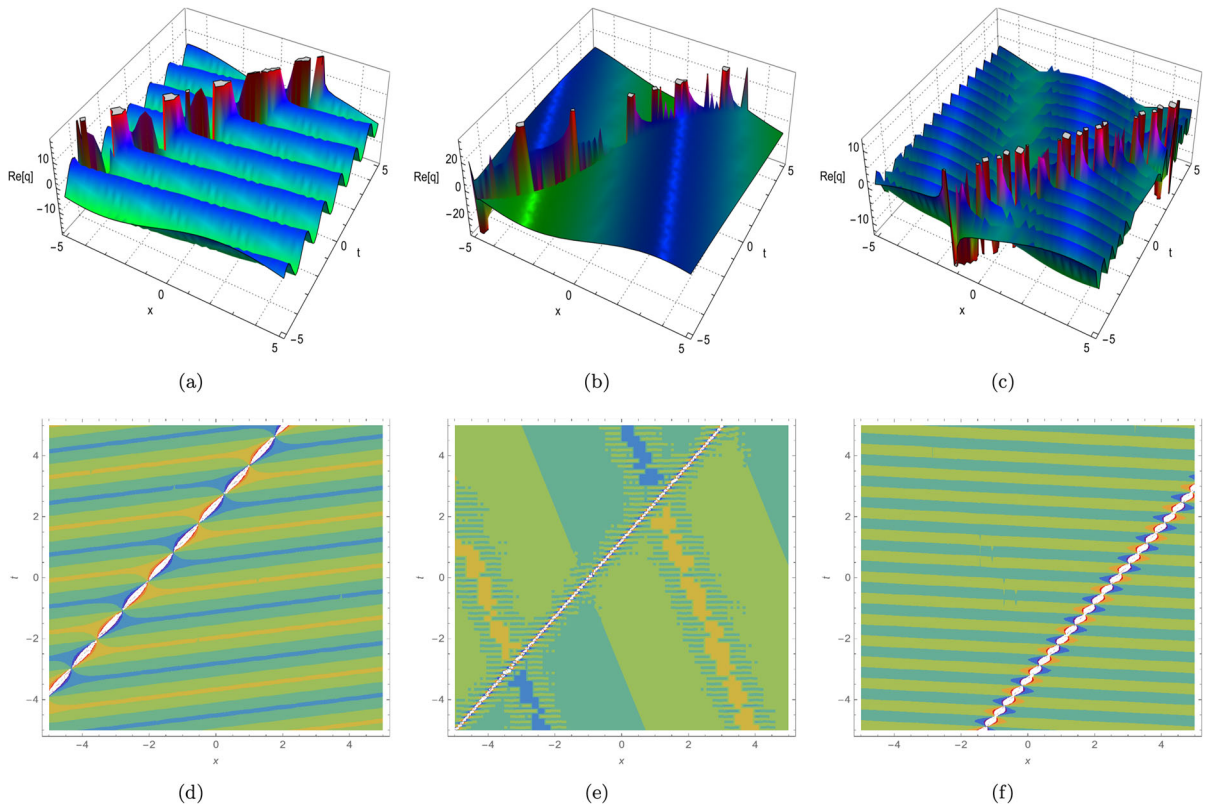


**Fig. 4** Dynamical behavior of solution (42)

$$\begin{aligned}
 M_4 &= -\frac{15}{2} - M_2 \left( \frac{3\chi_4^2}{\chi_1^2} + \frac{3\chi_5}{\chi_1^2 + \chi_3^2} \right), \\
 M_5 &= -8M_2, \quad M_6 = 2M_2 \left( \frac{\chi_4^2}{\chi_1^2} + \frac{\chi_5}{\chi_1^2 + \chi_3^2} \right), \\
 \chi_2 &= -\frac{\chi_3\chi_4}{\chi_1}.
 \end{aligned} \tag{48}$$

This results in the following solution:

$$\begin{aligned}
 q(x, t) &= \frac{4\chi_1^2 (\chi_1^2 + \chi_3^2) \xi}{(\chi_1^2 + \chi_3^2) (\chi_1^2 \xi^2 + \chi_4^2) + \chi_1^2 \chi_5} \\
 &\quad \exp \left[ i \left( -\kappa x + \omega t \right. \right. \\
 &\quad \left. \left. + \sigma W(t) - \sigma^2 t + \theta \right) \right].
 \end{aligned} \tag{49}$$

(iv)

$$\begin{aligned}
 M_1 = 0, \quad M_3 &= \frac{3\chi_1^4 + 4M_2\chi_1\chi_2\chi_3\chi_4 + \chi_3^2 [3\chi_3^2 - 2M_2(\chi_2^2 + \chi_5)] - 2\chi_1^2 [M_2(\chi_4^2 + \chi_5) - 3\chi_3^2]}{8(\chi_1^2 + \chi_3^2)^2}, \\
 M_4 &= -\frac{3(5\chi_1^4 - 4M_2\chi_1\chi_2\chi_3\chi_4 + \chi_3^2 [5\chi_3^2 + 2M_2(\chi_2^2 + \chi_5)] + 2\chi_1^2 [5\chi_3^2 + M_2(\chi_4^2 + \chi_5)])}{2(\chi_1^2 + \chi_3^2)^2}, \\
 M_5 = -8M_2, \quad M_6 &= \frac{2M_2 [(\chi_2\chi_3 - \chi_1\chi_4)^2 + (\chi_1^2 + \chi_3^2)\chi_5]}{(\chi_1^2 + \chi_3^2)^2}.
 \end{aligned} \tag{50}$$

Taking these results into consideration, the governing equation possesses the solution

$$\begin{aligned}
 q(x, t) &= \frac{4[\chi_1(\chi_1\xi + \chi_2) + \chi_3(\chi_3\xi + \chi_4)]}{(\chi_1\xi + \chi_2)^2 + (\chi_3\xi + \chi_4)^2 + \chi_5} \\
 &\quad \exp\left[i\left(-\kappa x + \omega t + \sigma W(t) - \sigma^2 t + \theta\right)\right].
 \end{aligned} \tag{51}$$

Figure 5 provides the dynamical behavior of Peregrine-like rational solution (51). In the (x, t)-plane, Fig. 5a, b, and c exhibit the 3D graphs, while Fig. 5d, e, and f enumerate the corresponding contour diagrams of Fig. 5a, b, and c. In this case, the values of the parameters are  $v = 1.1$ ,  $\theta = 3$ ,  $\kappa = 0.7$ ,  $\chi_2 = 3$ ,  $\chi_4 = 7$ ,  $W(t) = \frac{\sigma}{2}t$  when  $\sigma = 0$ ,  $\chi_1 = 4.2$ ,  $\chi_3 = 3.4$ ,  $\chi_5 = -125$ ,  $\omega = 4$  in (a) and (d),  $\sigma = 2$ ,  $\chi_1 = 2.4$ ,  $\chi_3 = -6.5$ ,  $\chi_5 = 7$ ,  $\omega = 1.5$  in (b) and (e),  $\sigma = 10$ ,  $\chi_1 = 4.7$ ,  $\chi_3 = 16.4$ ,  $\chi_5 = 75$ ,  $\omega = 53$  in (c) and (f).

From Fig. 5d, e, and f, one can clearly see that the pulse profile remains unchanged during evolution. This is one of the important properties of soliton, which is highly desired in practical applications.

### 8 Three-wave solutions

Based on the three-wave approach, the solution is structured as [50]

$$\begin{aligned}
 \psi &= \varrho_1 \exp(\chi_1\xi + \chi_2) + \exp[-(\chi_1\xi + \chi_2)] \\
 &\quad + \varrho_2 \cos(\chi_3\xi + \chi_4) + \varrho_3 \sin(\chi_5\xi + \chi_6)
 \end{aligned} \tag{52}$$

where  $\chi_j$  ( $1 \leq j \leq 6$ ) are constants. Inserting (52) into (13) and collecting the coefficients of

$\exp(\chi_1\xi + \chi_2)$ ,  $\exp[-(\chi_1\xi + \chi_2)]$ ,  $\cos(\chi_3\xi + \chi_4)$ ,  $\sin(\chi_3\xi + \chi_4)$ ,  $\cos(\chi_5\xi + \chi_6)$ ,  $\sin(\chi_5\xi + \chi_6)$ , and other terms, and solving the resulting system, the following results are acquired:

Set-1.

$$\begin{aligned}
 M_3 &= -\frac{M_1 + 4M_2\chi_1^2}{16\chi_1^4}, \\
 M_4 &= \frac{M_1}{4\chi_1^4} + \frac{M_2}{\chi_1^2} - 2M_6 - 6, \\
 M_5 &= -4(M_6 + 1)\chi_1^2 + \frac{M_1}{\chi_1^2} + 2M_2, \\
 \varrho_1 = \varrho_2 = 0, \quad \chi_5 &= i\epsilon\chi_1.
 \end{aligned} \tag{53}$$

Putting these parameter values into (52), and utilizing (2) along with (12), one gets the solution given by

$$\begin{aligned}
 q(x, t) &= \frac{2\chi_1 [\epsilon\varrho_3 \exp(\chi_1\xi + \chi_2) \cosh(\epsilon\chi_1\xi - i\chi_6) + i]}{\varrho_3 \exp(\chi_1\xi + \chi_2) \sinh(\epsilon\chi_1\xi - i\chi_6) - i} \\
 &\quad \exp\left[i\left(-\kappa x + \omega t + \sigma W(t) - \sigma^2 t + \theta\right)\right].
 \end{aligned} \tag{54}$$

Set-2.

$$\begin{aligned}
 M_3 &= -\frac{M_1 + 4M_2\chi_1^2}{16\chi_1^4}, \quad M_4 = \frac{M_1}{4\chi_1^4} + \frac{M_2}{\chi_1^2} \\
 &\quad - 2M_6 - 6, \quad M_5 = -4(M_6 + 1)\chi_1^2 + \frac{M_1}{\chi_1^2} \\
 &\quad + 2M_2, \quad \varrho_2 \\
 &= 0, \quad \chi_5 = i\epsilon\chi_1.
 \end{aligned} \tag{55}$$

From the solution set, it is procured that

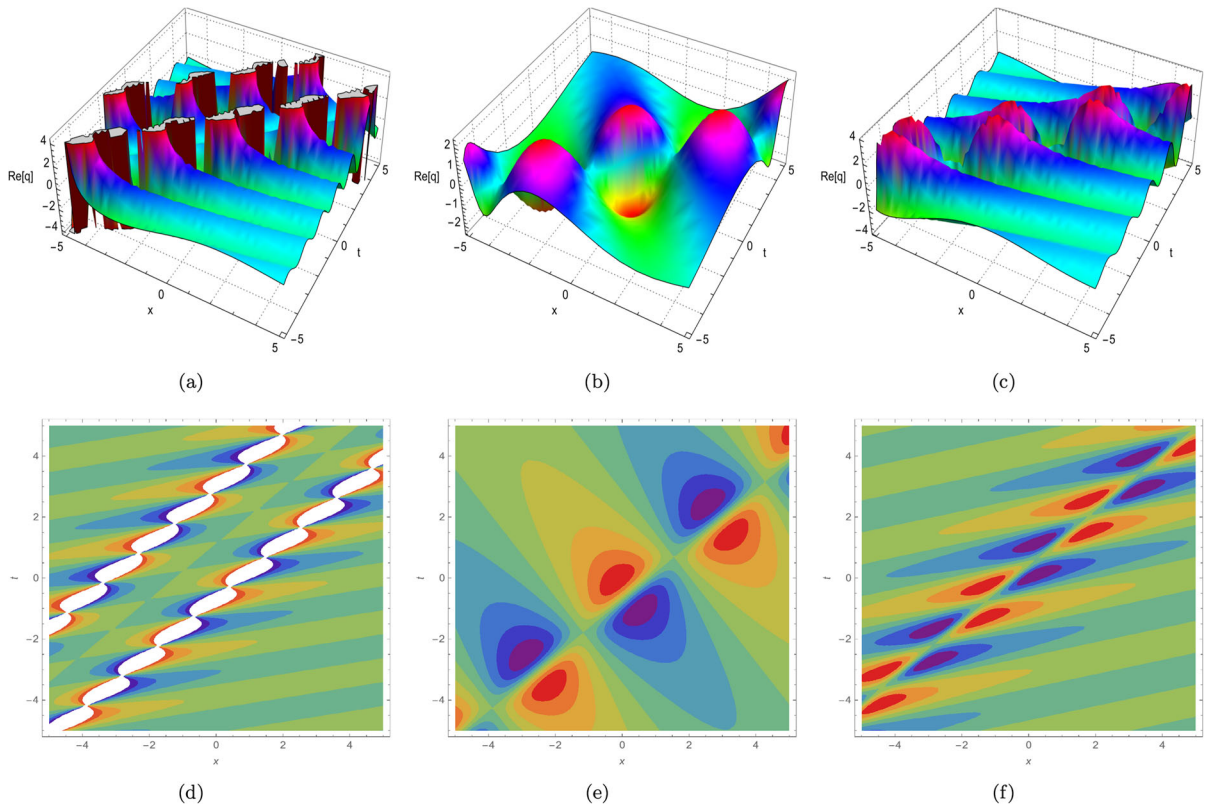


**Fig. 5** Dynamical behavior of solution (51)

$$q(x, t) = \frac{2\chi_1 [\varrho_1 \exp[2(\chi_1 \xi + \chi_2)] + i\epsilon \varrho_3 \exp(\chi_1 \xi + \chi_2) \cosh(\epsilon \chi_1 \xi - i\chi_6) - 1]}{\varrho_1 \exp[2(\chi_1 \xi + \chi_2)] + i\varrho_3 \exp(\chi_1 \xi + \chi_2) \sinh(\epsilon \chi_1 \xi - i\chi_6) + 1} \exp \left[ i \left( -\kappa x + \omega t + \sigma W(t) - \sigma^2 t + \theta \right) \right]. \tag{56}$$

From (54) and (56), it appears that these solutions remain valid as long as the constraint relations  $\varrho_3 = i\beta_1$  and  $\chi_6 = i\beta_2$  ( $\beta_1, \beta_2 \in \mathbb{R}$ ) hold.  
 Set-3.

$$\begin{aligned} M_5 &= -4(M_6 + 1)\chi_1^2 + \frac{M_1}{\chi_1^2} + 2M_2, \\ \varrho_1 &= 0, \quad \chi_3 = i\chi_1, \quad \chi_5 = i\epsilon\chi_1. \end{aligned} \tag{57}$$

Then, the solution falls out as

$$\begin{aligned} M_3 &= -\frac{M_1 + 4M_2\chi_1^2}{16\chi_1^4}, \\ M_4 &= \frac{M_1}{4\chi_1^4} + \frac{M_2}{\chi_1^2} - 2M_6 - 6, \end{aligned}$$

$$q(x, t) = \frac{2\chi_1 [\exp(\chi_1\xi + \chi_2) [\varrho_2 \sinh(\chi_1\xi - i\chi_4) + i\epsilon\varrho_3 \cosh(\epsilon\chi_1\xi - i\chi_6)] - 1]}{\exp(\chi_1\xi + \chi_2) [\varrho_2 \cosh(\chi_1\xi - i\chi_4) + i\varrho_3 \sinh(\epsilon\chi_1\xi - i\chi_6)] + 1} \exp\left[i\left(-\kappa x + \omega t + \sigma W(t) - \sigma^2 t + \theta\right)\right]. \tag{58}$$

Set-4.

$$\begin{aligned} M_3 &= -\frac{M_1 + 4M_2\chi_1^2}{16\chi_1^4}, \\ M_4 &= \frac{M_1}{4\chi_1^4} + \frac{M_2}{\chi_1^2} - 2M_6 - 6, \\ M_5 &= -4(M_6 + 1)\chi_1^2 + \frac{M_1}{\chi_1^2} + 2M_2, \quad \chi_3 = i\chi_1, \\ \chi_5 &= i\epsilon\chi_1. \end{aligned} \tag{59}$$

Finally, these outcomes yield the following three-wave solution:

$$q(x, t) = \frac{2\chi_1 [\exp(\chi_1\xi + \chi_2) [\varrho_1 \exp(\chi_1\xi + \chi_2) + \varrho_2 \sinh(\chi_1\xi - i\chi_4) + i\epsilon\varrho_3 \cosh(\epsilon\chi_1\xi - i\chi_6)] - 1]}{\exp(\chi_1\xi + \chi_2) [\varrho_1 \exp(\chi_1\xi + \chi_2) + \varrho_2 \cosh(\chi_1\xi - i\chi_4) + i\varrho_3 \sinh(\epsilon\chi_1\xi - i\chi_6)] + 1} \times \exp\left[i\left(-\kappa x + \omega t + \sigma W(t) - \sigma^2 t + \theta\right)\right]. \tag{60}$$

In all solution sets given here,  $\epsilon = \pm 1$ . Also, it needs to be mentioned that the solutions (58) and (60) remain valid under the conditions  $\varrho_3 = i\beta_1$ ,  $\chi_6 = i\beta_2$ , and  $\chi_4 = i\beta_3$ , where  $\beta_j (j = 1, 2, 3) \in \mathbb{R}$ .

The solution provided by Eq. (60) is depicted graphically in Fig. 6. In the (x, t)-plane, Fig. 6a, b, and c show the 3D graphs, while Fig. 6a, e, and f are the corresponding contour diagrams of Fig. 6a, b, and c. In Fig. 6, the parameter values are  $v = 1.8$ ,  $\epsilon = -1$ ,  $\theta = 4$ ,  $\kappa = 1$ ,  $\varrho_1 = 3$ ,  $\varrho_2 = 7$ ,  $\varrho_3 = 2i$ ,  $\chi_2 = 5$ ,  $\chi_4 = 9i$ ,  $\chi_6 = 11i$ ,  $W(t) = \frac{\sigma}{2}t$  when  $\sigma = 2$ ,  $\chi_1 = 0.3$ ,  $\omega = 72$  in (a) and (d),  $\sigma = 4$ ,  $\chi_1 = 1$ ,  $\omega = 7.77$  in (b) and (e),  $\sigma = 0$ ,  $\chi_1 = -0.53$ ,  $\omega = 3.9$  in (c) and (f). For various values of the parameters  $\sigma$ ,  $\chi_1$ , and  $\omega$ , the propagation characteristics of the three-wave solution provided by Eq. (60) are displayed in Fig. 6, along with the examination range  $-5 \leq x \leq 5$  and  $-5 \leq t \leq 5$ .

Before arriving at a conclusion, let us compare the obtained analytical solutions with the experimental

results of nonlinear waves found in optical contexts. Here, we compare for example the obtained Peregrine-like rational soliton (51) with the Peregrine soliton that is experimentally observed in optical fibers by Kibler et al. [51]. Different from the Peregrine soliton obtained within the framework of the cubic NLSE [51], the Peregrine-like rational solution presented here possess a nontrivial phase structure which depends crucially on the noise coefficient  $\sigma$  and includes the time-dependent function  $W(t)$ . This special form of the phase may lead to chirped pulses when the function  $W(t)$  do not exhibit a linear variation in time. There are a number of real-world applications for this interesting frequency-chirping property, including effective pulse amplifica-

tion or compression. It should be noted that only the two fundamental effects, namely group velocity dispersion and self-phase modulation nonlinearity, may be balanced for the Peregrine soliton to form in a pure Kerr optical medium. This is different from the findings of the current study, which show that for them to exist in the optical fiber, a balance between higher-order effects of different nature is necessary.

### 9 Conclusions

The present research discussed the effect of multiplicative white noise in the Itô sense on the analytic solutions of the concatenation model, which is the conjunction of the NLSE, LPD model, and SSE, along with the Kerr law nonlinear form of SPM and STD, in addition to perturbation terms of the Hamiltonian type. To achieve this, the direct test functions, which comprise a combination of exponential, trigonometric, hyperbolic, and

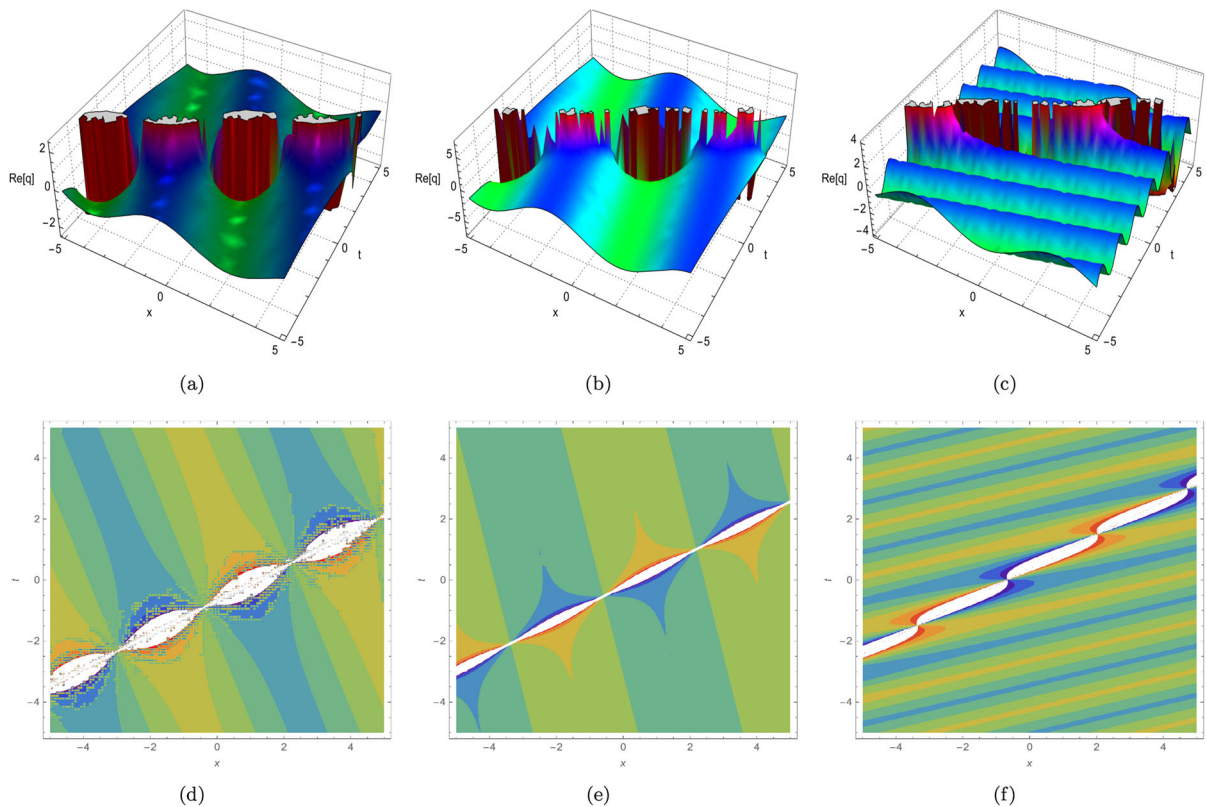


**Fig. 6** Dynamical behavior of solution (60)

quadratic functions, were implemented along with the Cole–Hopf transformation. The procedure continued with the extraction of multi-wave, two solitary wave, breather, periodic cross kink, Peregrine-like rational, and three-wave solutions for the perturbed stochastic concatenation model. The restrictions on the parameters essential for the existence of such solutions were also introduced. The interaction phenomenon of the recovered solutions is illustrated through 3D and contour graphics by assigning specific values to the parameters.

This study illustrates the potentially rich set of localized pulses and periodic waves in optical fiber media governed by the concatenation model. These results may be advantageous for further understanding of the nonlinear phenomena and dynamical processes arising in optical fibers and may be useful for experimental realization of undistorted transmission of nonlinear waves in optical waveguiding systems.

**Funding** Open access funding provided by the Scientific and Technological Research Council of Türkiye (TÜBİTAK). The authors have not disclosed any funding.

**Data availability** No data was used for the research described in the article.

#### Declarations

**Conflict of interest** The authors declare that there is no Conflict of interest.

**Open Access** This article is licensed under a Creative Commons Attribution 4.0 International License, which permits use, sharing, adaptation, distribution and reproduction in any medium or format, as long as you give appropriate credit to the original author(s) and the source, provide a link to the Creative Commons licence, and indicate if changes were made. The images or other third party material in this article are included in the article's Creative Commons licence, unless indicated otherwise in a credit line to the material. If material is not included in the article's Creative Commons licence and your intended use is not permitted by statutory regulation or exceeds the permitted use, you will need to obtain permission directly from the copyright holder. To view a copy of this licence, visit <http://creativecommons.org/licenses/by/4.0/>.



## References

1. Wazwaz, A.M.: Painlevé integrability and lump solutions for two extended (3+1)- and (2+1)-dimensional Kadomtsev–Petviashvili equations. *Nonlinear Dyn.* **111**(4), 3623–3632 (2023)
2. Ma, Y.L., Wazwaz, A.M., Li, B.Q.: New extended Kadomtsev–Petviashvili equation: multiple soliton solutions, breather, lump and interaction solutions. *Nonlinear Dyn.* **104**, 1581–1594 (2021)
3. Wazwaz, A.M.: Multi-soliton solutions for integrable (3+1)-dimensional modified seventh-order Ito and seventh-order Ito equations. *Nonlinear Dyn.* **110**(4), 3713–3720 (2022)
4. Wazwaz, A.M.: Integrable (3+1)-dimensional Ito equation: variety of lump solutions and multiple-soliton solutions. *Nonlinear Dyn.* **109**(3), 1929–1934 (2022)
5. Wazwaz, A.M.: Two new Painlevé integrable KdV–Calogero–Bogoyavlenskii–Schiff (KdV–CBS) equation and new negative-order KdV–CBS equation. *Nonlinear Dyn.* **104**(4), 4311–4315 (2021)
6. Xu, G.Q., Wazwaz, A.M.: Bidirectional solitons and interaction solutions for a new integrable fifth-order nonlinear equation with temporal and spatial dispersion. *Nonlinear Dyn.* **101**(1), 581–595 (2020)
7. Wazwaz, A.M., Xu, G.Q.: Kadomtsev–Petviashvili hierarchy: two integrable equations with time-dependent coefficients. *Nonlinear Dyn.* **100**, 3711–3716 (2020)
8. Wazwaz, A.M., Kaur, L.: New integrable Boussinesq equations of distinct dimensions with diverse variety of soliton solutions. *Nonlinear Dyn.* **97**, 83–94 (2019)
9. Liu, J.G.: Collisions between lump and soliton solutions. *Appl. Math. Lett.* **92**, 184–189 (2019)
10. Liu, J.G., Zhu, W.H., Zhou, L.: Multi-wave, breather wave, and interaction solutions of the Hirota–Satsuma–Ito equation. *Eur. Phys. J. Plus* **135**(1), 20 (2020)
11. Sun, Y.L., Chen, J., Ma, W.X., Yu, J.P., Khaliq, C.M.: Further study of the localized solutions of the (2+1)-dimensional B–Kadomtsev–Petviashvili equation. *Commun. Nonlinear Sci. Numer. Simul.* **107**, 106131 (2022)
12. Sun, H.Y., Zhaqilao: Rogue waves, modulation instability of the (2+1)-dimensional complex modified Korteweg–de Vries equation on the periodic background. *Wave Motion* **116**, 103073 (2023)
13. Ma, H., Mao, X., Deng, A.: Interaction solutions for the second extended (3+1)-dimensional Jimbo–Miwa equation. *Chin. Phys. B* **32**(6), 060201 (2023)
14. Feng, C.H., Tian, B., Yang, D.Y., Gao, X.T.: Lump and hybrid solutions for a (3+1)-dimensional Boussinesq-type equation for the gravity waves over a water surface. *Chin. J. Phys.* **83**, 515–526 (2023)
15. Liu, S., Yang, Z., Althobaiti, A., Wang, Y.: Lump solution and lump-type solution to a class of water wave equation. *Res. Phys.* **45**, 106221 (2023)
16. Gao, X.Y.: Oceanic shallow-water investigations on a generalized Whitham–Broer–Kaup–Boussinesq–Kupershmidt system. *Phys. Fluids* **35**(12), 127106 (2023)
17. Gao, X.Y.: Considering the wave processes in oceanography, acoustics and hydrodynamics by means of an extended coupled (2+1)-dimensional Burgers system. *Chin. J. Phys.* **86**, 572–577 (2023)
18. Gao, X.Y.: Letter to the Editor on the Korteweg–de Vries-type systems inspired by *Results Phys.* **51**, 106624 (2023) and **50**, 106566 (2023). *Res. Phys.* **53**, 106932 (2023)
19. Gao, X.Y.: Two-layer-liquid and lattice considerations through a (3+1)-dimensional generalized Yu–Toda–Sasa–Fukuyama system. *Appl. Math. Lett.* **152**, 109018 (2024)
20. Wu, X.H., Gao, Y.T.: Generalized Darboux transformation and solitons for the Ablowitz–Ladik equation in an electrical lattice. *Appl. Math. Lett.* **137**, 108476 (2023)
21. Shen, Y., Tian, B., Zhou, T.Y., Cheng, C.D.: Multi-pole solitons in an inhomogeneous multi-component nonlinear optical medium. *Chaos Solitons Fractals* **171**, 113497 (2023)
22. Zhou, T.Y., Tian, B., Shen, Y., Gao, X.T.: Auto-Bäcklund transformations and soliton solutions on the nonzero background for a (3+1)-dimensional Korteweg–de Vries–Calogero–Bogoyavlenskii–Schiff equation in a fluid. *Nonlinear Dyn.* **111**(9), 8647–8658 (2023)
23. Gao, X.T., Tian, B.: Water-wave studies on a (2+1)-dimensional generalized variable-coefficient Boiti–Leon–Pempinelli system. *Appl. Math. Lett.* **128**, 107858 (2022)
24. Ankiewicz, A., Wang, Y., Wabnitz, S., Akhmediev, N.: Extended nonlinear Schrödinger equation with higher-order odd and even terms and its rogue wave solutions. *Phys. Rev. E* **89**(1), 012907 (2014)
25. Ankiewicz, A., Akhmediev, N.: Higher-order integrable evolution equation and its soliton solutions. *Phys. Lett. A* **378**(4), 358–361 (2014)
26. Kudryashov, N.A., Biswas, A., Borodina, A.G., Yıldırım, Y., Alshehri, H.M.: Painlevé analysis and optical solitons for a concatenated model. *Optik* **272**, 170255 (2023)
27. Kudryashov, N.A., Kutukov, A.A., Biswas, A., Zhou, Q., Yıldırım, Y., Alshomrani, A.S.: Optical solitons for the concatenation model: power-law nonlinearity. *Chaos Solitons Fractals* **177**, 114212 (2023)
28. Biswas, A., Vega-Guzman, J., Kara, A.H., Khan, S., Triki, H., Gonzalez-Gaxiola, O., Moraru, L., Georgescu, P.L.: Optical solitons and conservation laws for the concatenation model. Undetermined coefficients and multipliers approach. *Universe* **9**(1), 15 (2023)
29. Tang, L., Biswas, A., Yıldırım, Y., Asiri, A.: Bifurcation analysis and chaotic behavior of the concatenation model with power-law nonlinearity. *Contemp. Math.* **4**(4), 1014–1025 (2023)
30. Yıldırım, Y., Biswas, A., Asiri, A.: A full spectrum of optical solitons for the concatenation model. *Nonlinear Dyn.* 1–18 (2023)
31. Yıldırım, Y., Biswas, A., Moraru, L., Alghamdi, A.A.: Quiescent optical solitons for the concatenation model with nonlinear chromatic dispersion. *Mathematics* **11**(7), 1709 (2023)
32. Tang, L., Biswas, A., Yıldırım, Y., Alghamdi, A.A.: Bifurcation analysis and optical solitons for the concatenation model. *Phys. Lett. A* **480**, 128943 (2023)
33. Kukkar, A., Kumar, S., Malik, S., Biswas, A., Yıldırım, Y., Moshokoa, S.P., Khan, S., Alghamdi, A.A.: Optical solitons for the concatenation model with Kudryashov’s approaches. *Ukr. J. Phys. Opt.* **24**(2), 155–160 (2023)
34. Gonzalez-Gaxiola, O., Biswas, A., Ruiz de Chavez, J., Asiri, A.: Bright and dark optical solitons for the concatenation model by the Laplace–Adomian decomposition scheme. *Ukr. J. Phys. Opt.* **24**(3), 222–234 (2023)

35. Adem, A.R., Biswas, A., Yıldırım, Y., Asiri, A.: Implicit quiescent optical solitons for the concatenation model with nonlinear chromatic dispersion and power-law of self-phase modulation by Lie symmetry. *J. Opt.* (in press)
36. Triki, H., Sun, Y., Zhou, Q., Biswas, A., Yıldırım, Y., Alshehri, H.M.: Dark solitary pulses and moving fronts in an optical medium with the higher-order dispersive and nonlinear effects. *Chaos Solitons Fractals* **164**, 112622 (2022)
37. Biswas, A., Vega-Guzman, J., Yıldırım, Y., Moraru, L., Iticescu, C., Alghamdi, A.A.: Optical solitons for the concatenation model with differential group delay: undetermined coefficients. *Mathematics* **11**(9), 2012 (2023)
38. Shohib, R.M.A., Alngar, M.E.M., Biswas, A., Yıldırım, Y., Triki, H., Moraru, L., Iticescu, C., Georgescu, P.L., Asiri, A.: Optical solitons in magneto-optic waveguides for the concatenation model. *Ukr. J. Phys. Opt.* **24**(3), 248–261 (2023)
39. Arnous, A.H., Biswas, A., Yıldırım, Y., Moraru, L., Iticescu, C., Georgescu, L.P., Asiri, A.: Optical solitons and complexitons for the concatenation model in birefringent fibers. *Ukr. J. Phys. Opt.* **24**(4), 4060–4086 (2023)
40. Arnous, A.H., Biswas, A., Yıldırım, Y., Asiri, A.: Quiescent optical solitons for the concatenation model having nonlinear chromatic dispersion with differential group delay. *Contemp. Math.* **4**(4), 877–904 (2023)
41. Zayed, E.M., Arnous, A.H., Biswas, A., Yıldırım, Y., Asiri, A.: Optical solitons for the concatenation model with multiplicative white noise. *J. Opt.* (in Press)
42. Liu, J.G., Zhu, W.H., Zhou, L., Xiong, Y.K.: Multi-waves, breather wave and lump-stripe interaction solutions in a (2+1)-dimensional variable-coefficient Korteweg-de Vries equation. *Nonlinear Dyn.* **97**, 2127–2134 (2019)
43. Liu, J.G., Xiong, W.P.: Multi-wave, breather wave and lump solutions of the Boiti–Leon–Manna–Pempinelli equation with variable coefficients. *Res. Phys.* **19**, 103532 (2020)
44. Ahmed, I., Seadawy, A.R., Lu, D.: Kinky breathers, W-shaped and multi-peak solitons interaction in (2+1)-dimensional nonlinear Schrödinger equation with Kerr law of nonlinearity. *Eur. Phys. J. Plus* **134**, 120 (2019)
45. Özkan, Y.S., Yaşar, E., Seadawy, A.R.: On the multi-waves, interaction and Peregrine-like rational solutions of perturbed Radhakrishnan–Kundu–Lakshmanan equation. *Phys. Scr.* **95**(8), 085205 (2020)
46. Ekici, M.: Kinky breathers, W-shaped and multi-peak soliton interactions for Kudryashov’s quintuple power-law coupled with dual form of non-local refractive index structure. *Chaos Solitons Fractals* **159**, 112172 (2022)
47. Ma, H., Zhang, C., Deng, A.: New periodic wave, cross-Kink wave, breather, and the interaction phenomenon for the (2+1)-dimensional Sharmo–Tasso–Olver equation. *Complexity* (2020)
48. Seadawy, A.R., Rizvi, S.T.R., Younis, M., Ashraf, M.A.: Breather, multi-wave, periodic-cross kink, *M*-shaped and interactions solutions for perturbed NLSE with quadratic cubic nonlinearity. *Opt. Quantum Electron.* **53**, 631 (2021)
49. Lu, D., Seadawy, A.R., Ahmed, I.: Peregrine-like rational solitons and their interaction with kink wave for the resonance nonlinear Schrödinger equation with Kerr law of nonlinearity. *Mod. Phys. Lett. B* **33**(24), 1950292 (2019)
50. Liu, J.G., Du, J.Q., Zeng, Z.F., Nie, B.: New three-wave solutions for the (3+1)-dimensional Boiti–Leon–Manna–Pempinelli equation. *Nonlinear Dyn.* **88**, 655–661 (2017)
51. Kibler, B., Fatome, J., Finot, C., Millot, G., Dias, F., Genty, G., Akhmediev, N., Dudley, J.M.: The Peregrine soliton in nonlinear fibre optics. *Nat. Phys.* **6**(10), 790–795 (2010)

**Publisher’s Note** Springer Nature remains neutral with regard to jurisdictional claims in published maps and institutional affiliations.